

Seven centuries of avalanche activity at Echalp (Queyras massif, southern French Alps) as inferred from tree rings

The Holocene
0(0) 1–13
© The Author(s) 2012
Reprints and permission:
sagepub.co.uk/journalsPermissions.nav
DOI: 10.1177/0959683612460784
hol.sagepub.com
SAGE

Christophe Corona,^{1,2} Jérôme Lopez Saez,² Markus Stoffel,^{1,3}
Georges Rovéra,⁴ Jean-Louis Edouard⁵ and Frédéric Berger²

Abstract

The purpose of this study was to reconstruct spatiotemporal patterns of avalanche events in a forested avalanche path of the Queyras massif (Echalp avalanche path, southeast French Alps). Analysis of past events was based on tree-ring series from 163 heavily affected multicentennial larch trees (*Larix decidua* Mill.) growing near or next to the avalanche path. A total of 514 growth disturbances, such as tangential rows of traumatic resin ducts, the onset of compression wood as well as abrupt growth suppression or release, were identified in the samples indicating 38 destructive snow avalanches between 1338 and 2010. The mean return period of snow avalanches was 22 years with a 4% probability that an avalanche occurs in a particular year. On a temporal plan, three maxima in snow avalanche frequency were reconstructed at the beginning of the 16th and 19th centuries and around 1850, correlating with below-average winter temperatures and glacier advances. Analysis of the spatial distribution of disturbed trees contributed to the determination of four preferential patterns of avalanche events. The comparison of dendrogeomorphic data with historical records demonstrate that at least 18 events – six of which were undocumented – reached the hamlet of Echalp during the last seven centuries, but no significant temporal trend was detected concerning the frequency of these extreme events.

Keywords

dendrogeomorphology, French Alps, frequency, multicentennial reconstruction, snow avalanche, tree-rings

Received 9 January 2012; revised manuscript accepted 15 July 2012

Introduction

To improve our knowledge of natural avalanche variability in the context of climate warming, sufficiently long data series are needed spanning periods for which conditions were different from today. In Alpine areas, some scarce chronicles date back to the 14th century (Fliri, 1998; Laely, 1984). However, as these records are usually related to events that had a direct impact on either property or human lives, they represent a partial record of the complete avalanche history (Casteller et al., 2011). On shorter timescales, using continuous observations, Schneebeli et al. (1997) investigated possible changes in the number of catastrophic avalanches around Davos, Switzerland, showing no modifications during the 20th century. Latenser and Schneebeli (2002) highlighted no changes in avalanche activity over the 1950–2000 period in Switzerland. Eckert et al. (2010a, 2010b) studied variations in avalanche occurrences in the northern French Alps, where changes in mean avalanche activity or in the number of winters with low or high activity vary only insignificantly over the last 60 years. Time series derived from lichenometric records (McCarroll, 1993; McCarroll et al., 1995), lake sediments (Nesje et al., 2007; Vasskog et al., 2011) or pollen counts (Blikra and Selvik, 1998) have showed an increase in avalanche frequency in northern and western Europe during the ‘Little Ice Age’. In the Massif des Ecrins (French Alps), Jomelli and Pech (2004) used lichenometry to demonstrate that avalanche magnitude has been declining since 1650. Yet, all of the above studies only yield data with relatively low resolution and are limited to study sites where depositional sequences have been conserved.

Where avalanche paths are covered with forest, dendrogeomorphology can be used to document past events and to complement written documents with annual resolution (Butler and Sawyer, 2008). The basic principles of tree-ring dating of mass-movement processes have been outlined, e.g. by Alestalo (1971), Butler (1987), Stoffel and Bollschweiler (2008) and Stoffel et al. (2010). Dendrogeomorphology is based on the fact that (1) trees form one increment ring per year in temperate climates and (2) that trees affected by geomorphic processes will record the event in the form of characteristic growth disturbances (GD) in their tree-ring series. The use of tree rings for the reconstruction of chronologies of snow avalanching has a decades-long history, with increasing sophistication characterizing most recent applications (Butler and Sawyer, 2008). Pioneering dendrogeomorphic studies on snow avalanches date back to the 1960s when Potter (1969) and

¹Université de Berne, Switzerland

²IRSTEA, UR EMGR, France

³University of Geneva, Switzerland

⁴Université Grenoble-I Joseph Fourier, UMR 5194-CNRS PACTE Territoires, France

⁵Centre Camille Julian UMR 6573 CNRS, Maison Méditerranéenne des Sciences de l’Homme, France

Corresponding author:

Christophe Corona, Université de Berne, Institut de géologie, Baltzerstrasse 1 + 3, Berne 3012, Switzerland.
Email: christophe.corona@dendrolab.ch

Schaerer (1972) developed the first avalanche reconstructions in North America (also see Table 1, Butler and Sawyer (2008) and Butler et al. (2010) for recent reviews). Dendrogeomorphic analyses of snow avalanches were unusual in Europe before the early 2000s but were becoming increasingly popular in the early 2000s (Table 1), particularly in the Alps (e.g. Casteller et al., 2007; Corona et al., 2010, 2012; Stoffel et al., 2006) and in the Pyrenees (Muntan et al., 2009).

To date, the longest dendrogeomorphic reconstructions cover 250 years (Table 1). They are mainly limited by the age of trees on avalanche paths. In this study, we provide a 700 yr dendrogeomorphic reconstruction of avalanche events for a slope of the Queyras Massif (French Alps) where multicentennial larch trees (*Larix decidua* Mill.) were apparently able to survive repeated avalanche activity. This high-resolution tree-ring record was then compared with an existing historic chronology to evaluate its accuracy. We finally examine the coincidence between fluctuations in avalanche frequency and historic climate data including temperature, precipitation and glacier fluctuations.

Study site

The Echalp avalanche path (44°45'N, 7°00'E) is located on the western slope of the Guil valley (Figure 1a), in the Queyras Regional Park, southeastern Briançonnais (Hautes Alpes, France). This path threatens the hamlet of Echalp (village of Ristolas, Figure 1b). At the study site, geology is dominated by the 'schistes lustrés' belt of the inner Alps (Lemoine and Tricart, 1986). Schists have the form of impervious, tectonised, frost-sensitive bedrock. The climate has a mixed montane-mediterranean-continental character (Touflan et al., 2010). According to the data from the nearby meteorological station of Saint-Véran (2125 m a.s.l.), annual temperature is 5.8°C (±5.5°C) for the period 1928–2007. During winter, mean air temperature for the coldest month (February) is –3°C. The annual precipitation amounts to 900 mm (s.d. = 192 mm). Between October and May, precipitation falls primarily as snow. Average annual snowfall reaches 320 cm (±183 cm) for the period 1928–2007.

Snow avalanches released spontaneously from a starting zone located between 2100 and 2450 m a.s.l. (mean slope: 36°). Once released, they pass through a central track (mean slope: 32°, path length: 1200 m) before reaching the runout zone (mean slope: 15°) at 1750 m a.s.l. A topographic berm (20°) is observed between 1900 and 2100 m a.s.l. A characteristic transverse vegetation pattern (Malanson and Butler, 1984) can be observed across the track: the inner zone is colonized by shrubs and shade-intolerant pioneer tree species such as European rowan (*Sorbus aucuparia* L.), silver birch (*Betula pendula* Roth.) and juniper (*Juniperus sibirica* Burgsd.). In the outer zone, the forest vegetation is comprised mainly of European larch (*Larix decidua* Mill.), situated at altitudes between 1700 and 2400 m a.s.l. (Touflan et al., 2010, Figure 1d). The understorey is dominated by herbaceous species and shrubs, namely *Rhododendron ferrugineum* L. (rhododendron) and *Vaccinium myrtillus* L. (bilberry).

On this path, archival data refer to 12 catastrophic avalanche events (Table 2) with fatalities or damage to infrastructure in the hamlet of Echalp between AD 1408 and 1946 (Le Gallou and Guignard, 2011; Tivollier and Isnel, 1938). The last one in 1946 killed ten people and destroyed four houses and the chapel (Figure 1c).

Material and methods

Dendrogeomorphic analysis

The reactions of trees to snow avalanches are driven by the forces of the avalanche and the mechanical impact of debris (i.e. rocks and boulders or broken trees) transported by the snow, as well as

by the size and flexibility of the tree itself (Bebi et al., 2009). Typical morphologies of avalanche trees include tilting, wounding as well as trunk, apex and branch breakage (Bartelt and Stöckli, 2001; Luckman, 2010; Figures 1d and 2). These external anomalies are reflected in the wood through anomalous anatomical features, which can be detected and accurately dated in tree-ring series using dendrogeomorphic techniques (e.g. Stoffel and Bollschweiler, 2008, 2009).

The reactions most commonly observed in tree rings following avalanche activity are (1) a distinct growth suppression (Butler and Malanson, 1985) following apex loss or the break off of branches (Johnson, 1987), (2) the formation of compression wood (Timell, 1986) with thicker (rounder) and slightly darker tracheids (Stoffel and Bollschweiler, 2008) after tilting, and (3) the production of chaotic callus tissue (Stoffel et al., 2010) and tangential rows of traumatic resin ducts (referred hereafter as to TRD) at the edges of the injury after wound infliction and/or cambium damage (Schneuwly et al., 2008; Stoffel and Hitz, 2008). For this investigation, we used the appearance of callus tissue and TRD, the initiation of compression wood and abrupt growth reductions to determine the occurrence of avalanches.

A total of 163 *L. decidua* trees was sampled with 366 increment cores. A minimum of two cores were extracted per tree, one perpendicular to the slope and one in the downslope direction. GPS coordinates were recorded for each tree with 1 m accuracy using a Trimble GeoExplorer. For each tree, additional data were collected, including its position within the avalanche track, its diameter at breast height (DBH), description of the disturbance (i.e. amount of impact scars, branch flagging, and tilting) and information on neighboring trees. Sampling height was chosen according to the morphology of the stem: (1) injured or tilted trees were sampled at the height of the disturbance; (2) cross-sections and cores from decapitated trees were, in contrast, extracted next to the stem base so as to preserve as much tree-ring information as possible (Stoffel and Bollschweiler, 2008).

In addition to the disturbed trees sampled in the path, (3) 24 undisturbed *L. decidua* trees showing no signs of avalanche activity or any other geomorphic process were selected outside of the active avalanche zone. Two cores were extracted per tree, two perpendicular to the slope and one in the downslope direction. The preparation and analysis of samples followed standardized geomorphic procedures as described in Stoffel and Bollschweiler (2008). Ring-width measurements were made with a digital LINTAB positioning table with an adjoining Leica stereomicroscope and the time-series analysis software TSAP (Rinntech, 2009). Resulting measurements were graphically and statistically compared with the reference chronology computed from undisturbed trees using COFECHA (Holmes, 1983); missing or false rings were corrected where necessary. For samples heavily impacted by multiple avalanches, marker years recorded in neighboring samples were used to ensure accurate calendar dating (Reardon et al., 2008). Thereafter, all samples were visually inspected under a stereomicroscope to identify GD.

Tree-ring reconstruction of avalanches

In a subsequent step, we assigned scores to each avalanche-related GD using an approach similar to those used previously by Dubé et al. (2004), Reardon et al. (2008) or Corona et al. (2010):

- Intensity 5: Abrupt change in radial growth associated with stem breakage; or clear impact scar associated with obvious compression wood or TRD or growth suppression.
- Intensity 4: Clear scar, but no compression wood or suppression of growth or obvious compression wood that lasts for approximately three years.

Table 1. Bibliographic synthesis on tree-ring reconstructions of snow avalanches.

Country	Localisation	Number of paths	Species	Sample depth	Period	No. of growth disturbances	Minimal Index value	No. of avalanche events
USA	Wyoming			17				
Canada	British Columbia	Unknown	Unknown	Unknown	Unknown	Unknown	Unknown	Unknown
USA	Washington	13	Unknown	Unknown	Unknown	Unknown	Unknown	Unknown
USA	Colorado	Unknown	<i>Populus tremuloides</i> , <i>Picea engelmannii</i>	Unknown	1860–1974	56	Unknown	6
USA	Colorado	1	<i>Populus tremuloides</i> , <i>Picea engelmannii</i> , <i>Abies lasiocarpa</i>	50	1880–1976	Unknown	Unknown	4
USA	Montana	5		30				
USA	Montana	2	<i>Picea engelmannii</i> , <i>Abies lasiocarpa</i> , <i>Pseudotsuga menziesii</i> , <i>Larix occidentalis</i> , <i>Pinus contorta</i>	30 + 48	1924–1979 1934–1981	Unknown	40%	10+15
Canada	Alberta							
Canada	Alberta							
USA	Colorado	3	<i>Populus tremuloides</i> , <i>Picea engelmannii</i>	60 + 60 + 60	Unknown	Unknown	Unknown	Unknown
USA	Wyoming							
USA	Colorado	2						
Canada	Québec	1	<i>Picea glauca</i> , <i>Picea mariana</i> , <i>Abies balsamea</i> , <i>Larix laricina</i>	111	1885–2000	Unknown	10%	3
USA	Utah	16	<i>Picea engelmannii</i> , <i>Abies lasiocarpa</i>	297 (8–26)	1928–1996	Unknown	Unknown	14
Canada	Québec	1	<i>Abies balsamea</i> , <i>Picea mariana</i>	62	1895–1996	Unknown	10%	35
USA	Utah	1	<i>Picea engelmannii</i> , <i>Abies concolor</i> , <i>Populus tremuloides</i>	78	1891–1995	Unknown	Unknown	13
Canada	Québec	3	<i>Thuja occidentalis</i> , <i>Abies balsamea</i> , <i>Betula papyrifera</i>	62+20+28	1871–1996	Unknown	10%	7
Spain	Pyrenees	1	<i>Pinus uncinata</i>	230	1750–2000	Unknown	Unknown	3
Japan		1	<i>Abies mariesii</i>	34	Unknown	Unknown	not computed	not computed
Canada	Québec	2	Unknown	78 + 52	1941–2004	420	Unknown	11
USA	Montana	1	<i>Pseudotsuga menziesii</i>	109	1910–2003	Unknown	10%	27
Switzerland	Alps	1	<i>Larix decidua</i>	251	1750–2002	561	Unknown	9
Switzerland	Alps	2	<i>Larix decidua</i> , <i>Picea abies</i>	66 + 79	Unknown	Unknown	not computed	not computed
Argentina	Andes	1	<i>Nothofagus pumilio</i>	20	Unknown	Unknown	not computed	not computed
USA	Colorado	2	<i>Abies lasiocarpa</i> , <i>Pseudotsuga menziesii</i> , <i>Pinus contorta</i>	10+12	1945–2008 1963–2008	Unknown	20%, 40%	15 + 9
USA	Montana	1	<i>Pseudotsuga menziesii</i>	109	1910–2003	Unknown	10%	27
Canada	Québec	12	Unknown	10–243	1895–1999	51–799	10%	19
India	Himalaya	1	<i>Cedrus deodara</i>	36	1972–2006	Unknown	Unknown	4
Argentina	Andes	1	<i>Nothofagus pumilio</i>	50	Unknown	Unknown	Unknown	6
Spain	Pyrenees	6	<i>Pinus uncinata</i>	26–131	1870–2000	Unknown	16–40%	3
France	Alps	1	<i>Larix decidua</i>	232	1919–1994	901	10	20
Turkey	Kayaarka	2	<i>Abies bornmuelleriana</i>	61	Unknown	Unknown	not computed	not computed
Argentina	Andes	9	<i>Nothofagus pumilio</i>	6–15	1820–2005	Unknown	Unknown	6

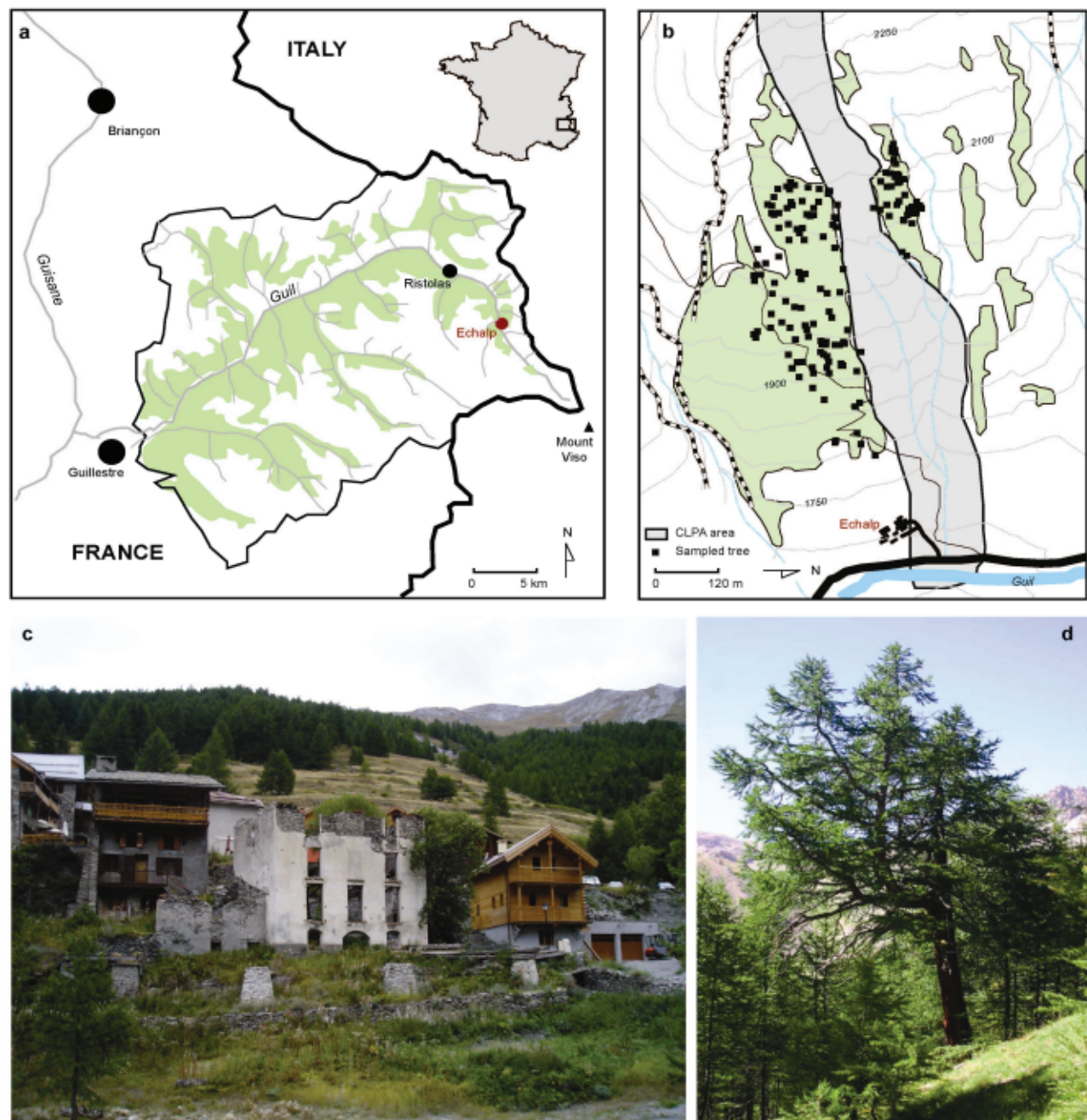


Figure 1. The upper Guil valley (a) and the Echalp avalanche path (b); houses hit and partly damaged by the avalanche event of 1946 in the hamlet of Echalp (c) and candelabra growth in multicentennial trees disturbed by past snow avalanches.

Table 2. Recorded avalanches that have caused damage on the Echalp avalanche path.

Date of event	Damage	Source
1408 and/or 1419	18 persons killed, 20 houses destroyed	Le Gallou and Guignard (2011)
1487	12 persons killed, 18 houses destroyed	Tivollier and Isnel (1938)
1681	15 persons killed in hamlets and villages of the Queyras massif, Echalp, Ristolas, Abriès and Molines	Le Gallou and Guignard (2011)
1706	Several houses destroyed	Le Gallou and Guignard (2011)
1791	2 persons killed, 11 houses damaged	Le Gallou and Guignard (2011)
1792	1 person killed, 5 houses destroyed	Le Gallou and Guignard (2011)
1855	6 persons killed, 5 houses destroyed	Le Gallou and Guignard (2011)
1861	6 houses destroyed	Le Gallou and Guignard (2011)
1885	5 houses destroyed, 14 houses damaged	Le Gallou and Guignard (2011)
1889	12 houses destroyed	Tivollier and Isnel (1938)
1895	6 houses damaged	Le Gallou and Guignard (2011)
1946	10 persons killed, 4 houses and the chapel destroyed	Le Gallou and Guignard (2011)

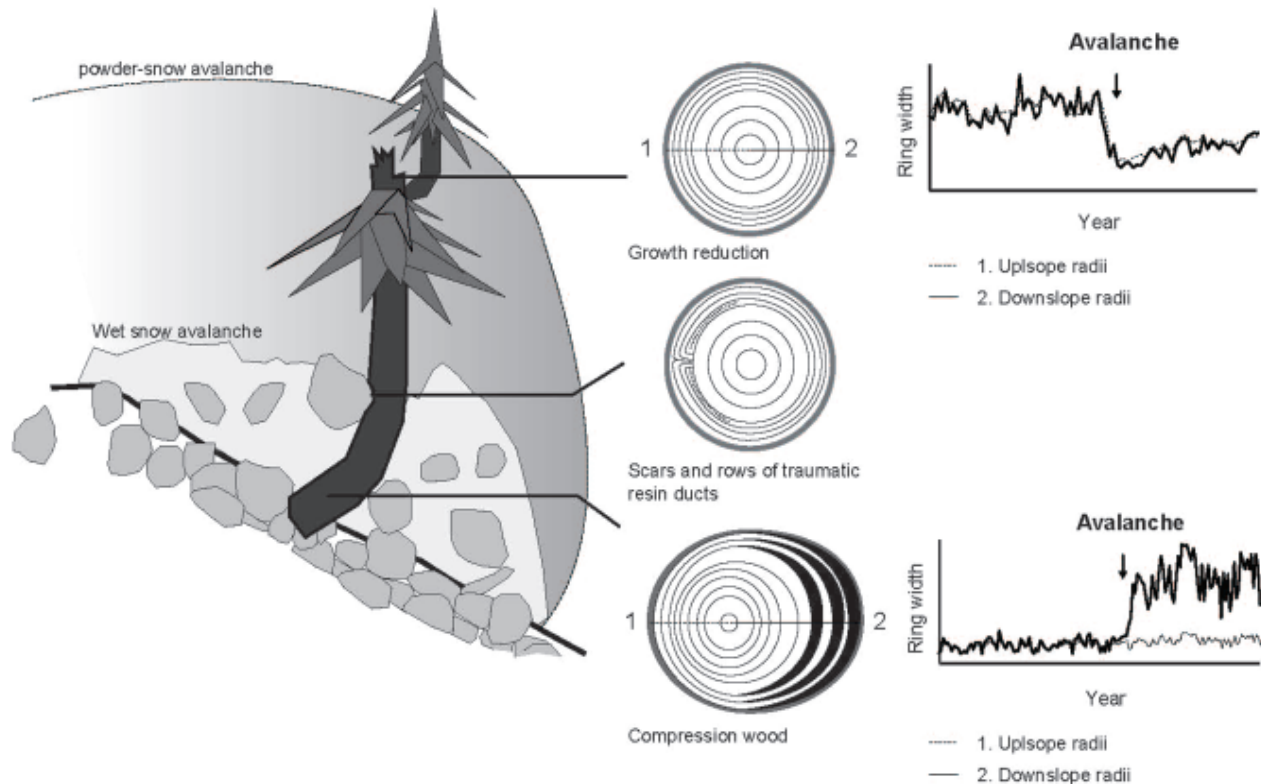


Figure 2. Dendrogeomorphic evidence used to infer avalanche events.

- Intensity 3: Obvious compression wood during 1 or 2 successive growth years following the disturbance.
- Intensity 2: Compression wood or growth suppression present but not well defined; or compression wood present but formed when the tree was young and more susceptible to damage from various environmental and biological factors.
- Intensity 1: Same as intensity 2 except that compression wood is very poorly defined, and slow onset may indicate other processes such as soil or snow creep as the primary causes of disturbance.

This rating system emphasizes features that are clearly associated with avalanche activity and discriminates against disturbances which can be induced by a variety of factors other than snow avalanches (e.g. improved light conditions or creeping snow). GD data from individual trees were then summarized in event response histograms (Dubé et al., 2004; Reardon et al., 2008; Shroder, 1980).

For each year t , an index I was calculated based on the percentage of trees showing responses in their tree-ring record in relation to the number of trees sampled being alive in year t :

$$I_t = \left(\frac{\sum_{i=1}^n (Rt)}{\sum_{i=1}^n (At)} \right) * 100 \quad (1)$$

where R represents the response of a tree to an event in year t and A the number of trees available in year t . As a result of the large sample size (Butler and Sawyer, 2008) available in the present study, the chronology of high-magnitude avalanches was based on an Index number I of 5% of all samples alive at year t . This threshold minimizes the risk that growth anomalies caused by other (geomorphic) processes could mistakenly be attributed to avalanches. We also required that a minimum of five trees exhibit

a response so as to avoid an overestimation in the calculation of response percentage resulting from a low number of trees early in the record (Dubé et al., 2004). A major avalanche was though considered as an event with $I_t > 5\%$ and which causes GD to at least five trees.

However, the strictness of these thresholds and the large sample size may induce a misclassification of minor events. To avoid misclassification, the yearly patterns of disturbed trees for years with $5\% \geq I_t > 2\%$ and GD in at least five trees were carefully examined. Using geographical coordinates, trees were placed into a Geographical Information System (GIS; ArcGIS 9.3) as geo-objects, and years of GD were linked as attributes to each single tree. We computed autocorrelations (feature similarity) based on the location and values of trees with the ArcGIS pattern analysis module and calculated yearly Moran indices (Moran, 1950) to evaluate whether the pattern of disturbed trees was clustered, dispersed or random. A Moran index value near 1 indicates clustering while a value near -1 indicates dispersion. Random and dispersed patterns were disregarded from the reconstruction whereas years with clustered patterns were considered as minor or spatially limited movements (Corona et al., 2010).

Climate influence on avalanche frequency

Avalanches should respond quickly to meteorologic and climatic variations, as they occur at altitudes close to the 0°C isotherm in mountain environments. We have thus hypothesized that avalanche regimes may be a good indicator of recent and past winter climatic conditions. To test this hypothesis, the newly developed reconstruction of past avalanche events was compared with: (1) length variations for the Lower Grindewald (Holzhauser et al., 2005) and the Mer de Glace (Zumbühl et al., 2008) glaciers at the decadal scale; (2) historical indices from Pfister (1993) (Pfister93) and (3) meteorological gridded data from Böhm et al. 2010 (Böhm10). The glacier length fluctuations for the Low Grindewald

glacier and for the Mer de Glace glaciers were reconstructed with a wealth of different historical sources (e.g. drawings, paintings, prints, photographs, maps). They cover the period 1520–2003 and 1550–2008, respectively. The Pfister93 graduated indices of winter temperatures and precipitations (1525–1990) cover central Europe and are related to biological indicators and historical archives. Monthly graduated indices (GI) range from -3 to $+3$ (from extremely cold to extremely warm anomalies), with 0 being ‘average’ months (according to the 1901–1960 period) or unavailable data. On a seasonal level the GI is defined as the average of the monthly GI, which yields gradations of 0.3 between -3 and $+3$.

The Böhm10 data set was extracted from the HISTALP data base. This data set, resulting from a dense network of 134 meteorological stations, covers the Greater Alpine Region (GAR: $4-19^{\circ}\text{E}$, $43-49^{\circ}\text{N}$, $0-3500$ m a.s.l.). It consists of station data gridded at $1^{\circ} \times 1^{\circ}$ ($0.1^{\circ} \times 0.1^{\circ}$), latitude \times longitude, representing temperature (precipitation) deviations from the 1961–1990 mean. It extends back to 1760 for temperature and 1800 for precipitations. Here, for the purpose of comparison with the avalanche reconstruction, a December–April mean series was calculated from four HISTALP point values enclosing the study site.

Results

Age structure of the stand

The reference chronology covers the period 1338–2010. Visual cross-dating was carried out by means of the skeleton plot method and primarily based on the narrow rings of 1500, 1643, 1668, 1741 and 1906 (Figure 3). After cross-dating, data on the pith age at breast height indicates that the 163 trees sampled on the Echalp path are on average 402 years old (± 143 years). The oldest tree selected for analysis attained sampling height in 1353 while the youngest reached breast height in 1897. A total of 52 trees were at least 500 years old. As can be seen in Figure 4, the distribution of disturbed multicentennial larches on the slope is homogeneous. This distribution of oldest trees suggests that no catastrophic event destroyed large parts of the stand during the past 700 years.

Reconstruction of avalanche events

The 366 increment cores selected from the 163 trees permitted identification of 553 GD mostly relating to past snow avalanche activity. Table 3 illustrates the nature of GD as well as their intensity. Abrupt growth reductions were the GD most frequently identified in the samples (224, 41%), followed by TRD (209, 38%), callus tissue (40, 7%) and compression wood (80, 14%). In total, 66% of the GD were rated severe, high-intensity disturbances (intensity classes 4 or 5). The oldest GD identified in the tree-ring series was dated to 1387. GD became more frequent

after 1620, and GD have been observed in most year ever since (Figure 5a, b).

In total, 42 years exceeded the 2% threshold for It (Figure 5b) with at least five trees exhibiting a response (Figure 5a) between 1447 and 2010. A total of 33 major avalanche events with $GD > 5$ and $It > 5\%$ (Dubé et al., 2004; Germain et al., 2009; Reardon et al., 2008) were reconstructed, namely in: 1447, 1456, 1475, 1487, 1514, 1534, 1557, 1583, 1587, 1595, 1600, 1642, 1681, 1706, 1740, 1774, 1791, 1802, 1810, 1813, 1817, 1820, 1846, 1851, 1855, 1861, 1867, 1905, 1909, 1935, 1946, 1971 and 1974. The years 1909 ($n=36$), 1740 ($n=27$), 1810 ($n=24$) and 1935 ($n=16$) are those exhibiting the largest number of trees with GD (Figure 5a). In a similar way, the largest frequency of appearance of trees with GD was measured in 1909 (22%), 1740 (20%), 1447 (19%) and 1487 (17%) (Figure 5b). In contrast, for the years 1621, 1661, 1666, 1685, 1721, 1866, 1895, 1902 and 1940, the number of GD was > 5 and $5\% > It > 2\%$ and did not allow for them being considered avalanche events with equal confidence. The yearly Moran I statistics computed for these years vary between -0.05 in 1902 (i.e. dispersed distribution of affected trees) and 0.28 in 1666 (i.e. spatial clustering of GD). Five years (1621, 1666, 1685, 1721, 1895) display clustered patterns of disturbed trees with sufficient aggregation and were therefore considered avalanche events, as well. In 1661, 1866, 1902 and 1940 the spatial distribution of disturbed trees does not display any significant pattern and these years were not therefore kept for further analysis.

Considering the period since AD 1447, the overall return period (i.e. the average number of years between two events) is 15 years and the mean decadal frequency is 1.5 events. This value slightly increases from 14 years for the period 1447–1899 to 18 years for the period 1900–2010. Maximum decadal frequencies are observed in 1583–1600 (four events), 1802–1820 (five events) and 1846–1867 (five events). Conversely, no event was reconstructed for the periods 1487–1514, 1557–1583, 1642–1666, 1740–1774, 1820–1846, 1867–1905, and since 1974.

Spatial distribution of trees affected by avalanche events

The spatial distribution of trees affected by the same event is of considerable help for the determination of the minimum spatial extent of past avalanches. The reconstructed maps, provided in Figure 6, clearly indicate that the extent of the events varies according to four general patterns: (1) 11 major events (32%) affected trees located throughout the slope (Figure 6a,b) in 1487, 1681, 1706, 1740, 1774, 1791, 1846, 1851, 1855, 1909 and 1946; (2) a majority of events (49%) stopped at the topographic berm at 1900 m a.s.l. (Figure 6c) in 1447, 1475, 1514, 1557, 1587, 1595, 1642, 1666, 1685, 1721, 1810, 1813, 1817, 1820, 1861, 1895,

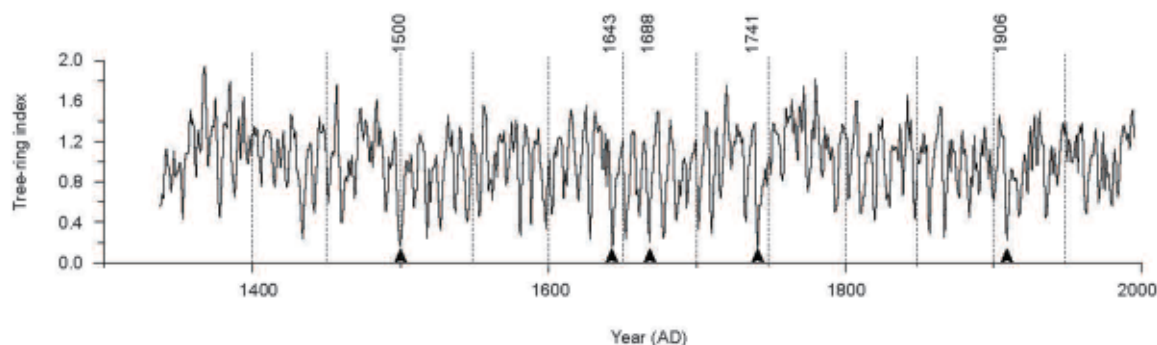


Figure 3. Tree-ring chronology of multicentennial European larch (*Larix decidua* Mill.) trees for the upper Guil valley dating back to AD 1338. Individual series are detrended with (1) a negative exponential curve or a linear regression and (2) by a cubic smoothing spline function.

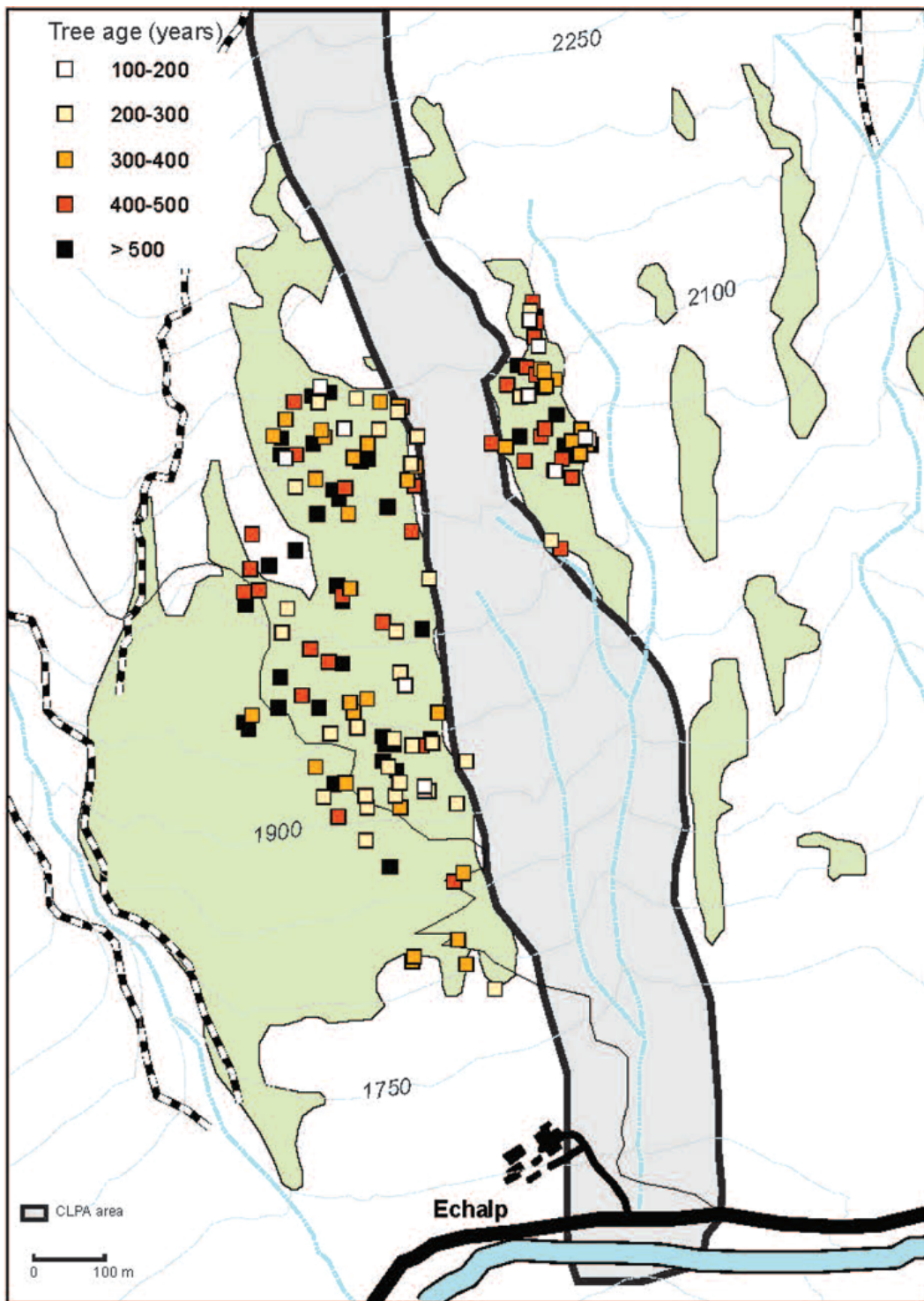


Figure 4. Age structure of the forest stand growing in and next to the Echalp avalanche path.

Table 3. Intensity reactions and types of growth disturbances (GD) assessed in the 163 trees selected for analysis.

Intensity	Number	%	Type	Number	%
1	37	7	Tangential rows of traumatic resin ducts	209	38
2	79	14	Compression wood	80	14
3	72	13	Callus tissue	40	7
4	56	10	Growth reduction	224	41
5	309	56			
Total	553	100		553	100

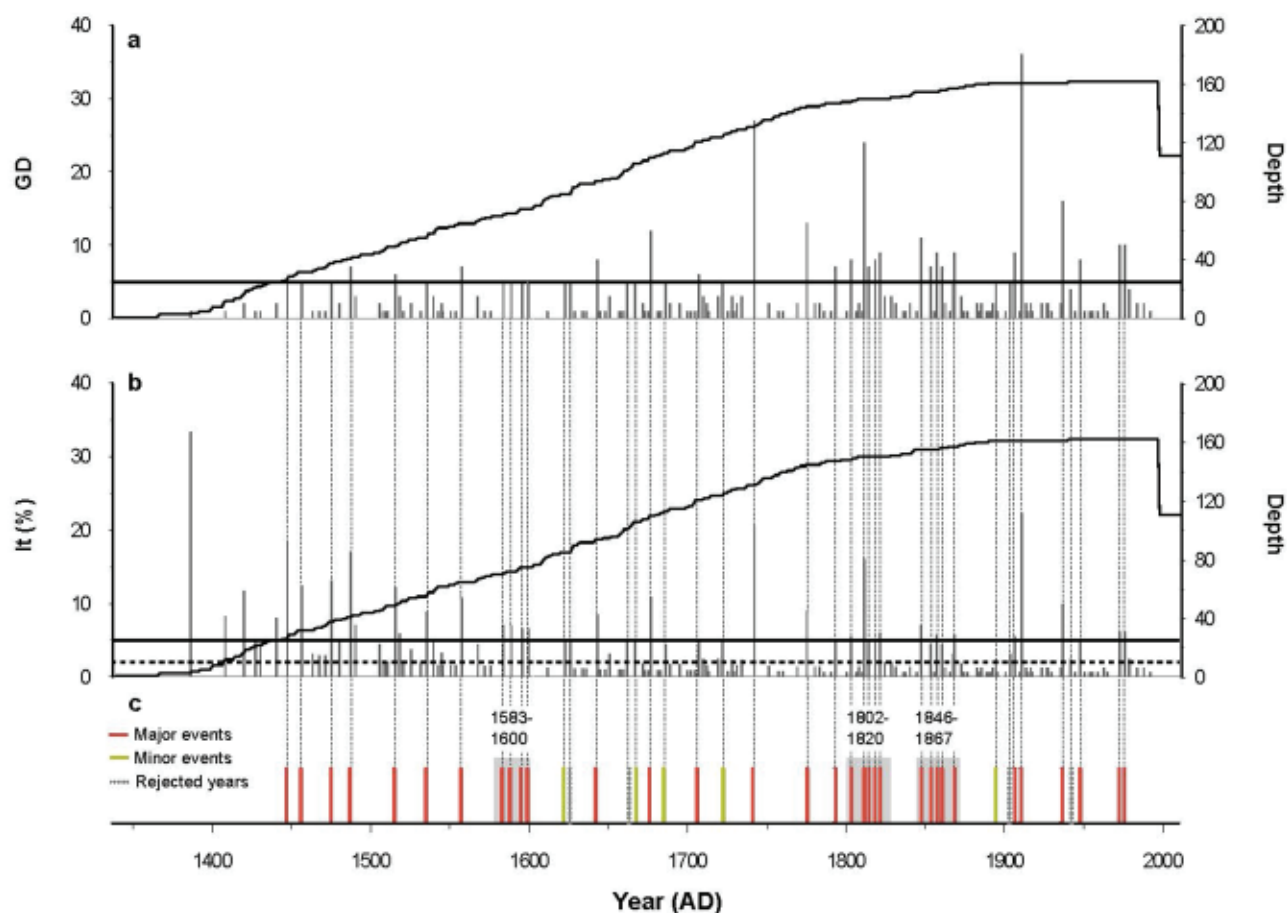


Figure 5. Event-response histograms showing avalanche-induced growth responses from sampled trees: (a) total number of growth disturbances (GD), (b) percentage of trees responding to an event and (c) avalanche events reconstructed for the period 1338–2010. Grey rectangles denote periods with high avalanche activity. The horizontal lines denote the GD (a) and It (b) thresholds used to reconstruct past minor (dotted line) and major (full lines) avalanche events.

1905, 1935 and 1974; (3) the events in 1583, 1802, 1867 and 1971 (10%), in contrast, only affected trees located on one side of the slope (Figure 6d); four minor events (1456, 1534, 1600, 1621, 10%) were restricted to the upper parts of the slope (>1900 m a.s.l.). Finally, it can also be seen from Figure 6 that reconstructed avalanche events frequently exceeded the lateral limits of the official map from the French Government localizing the occurrence of avalanches at the study site (Carte de Localisation des Phénomènes Avalancheux; hereafter referred to as CLPA).

Snow avalanches–climate relationships

The decadal avalanche variability at the Echalp path partially matches with climate histories inferred from glacier length fluctuations in the northern and central Alps (Figure 7a). Periods of high avalanche activity reconstructed in 1583–1600 (four events), 1802–1820 (five events) and 1846–1861 (four events) are in concert with glacier advances in the northern Alps and in Switzerland. Conversely, several periods with low avalanche activity, namely in 1557–1583, 1740–1774, 1867–1905 and 1974–2010, coincide with phases of important glacier retreats. At the annual scale, and when comparing our data with Pfister93, for the period 1525–1994, only six out of the 33 reconstructed events occurred during winters with temperature indices >1 (i.e. 1791, 1817, 1935, and 1974).

Conversely, 21 years were characterized by low winter temperatures with indices ≤ -1 . Seven events occurred during ‘extremely cold winters’, with indices ≤ -2 (i.e. 1534, 1587, 1595, 1600, 1681, 1810, and 1895). Additionally, 14 years were characterized by ‘very cold’ winters, with indices ranging between -2

and -1 , namely in 1557, 1621, 1642, 1666, 1685, 1740, 1802, 1813, 1820, 1851, 1855, 1861, 1909, 1971.

A comparison with the Böhm10 data set confirms the influence of negative temperature anomalies for the period 1760–2007 as 15 out of 19 reconstructed avalanche events are associated with negative temperature anomalies. Lowest temperatures ($< -1^\circ\text{C}$ compared with the 1961–1990 mean) were reported in 1774 (-1.5°C), 1802 (-1.7°C), 1813 (-2.8°C), 1820 (-1°C), 1846 (-2.5°C), 1851 (-1°C), 1855 (-1°C), 1861 (-1.5°C), 1867 (-1.8°C), 1895 (-1°C), 1905 (-1°C) and 1946 (-3.1°C). Conversely, no systematic synchronism was detected between our reconstruction and winter precipitation neither when comparing our series with that of Pfister93 nor that of Böhm10.

Discussion

Temporal accuracy of the reconstruction

The reconstruction complemented the existing avalanche chronology back to 1447 and added 31 events which were previously unknown. Seven of the reconstructed avalanche years between 1447 and 2010 (1487, 1681, 1706, 1791, 1855, 1861 and 1946) are listed in historical archives. Two other events are indirectly confirmed via historical data on intense avalanche activity in the Queyras region, namely the avalanches of 1909 and 1974 (MEDD, CEMAGREF, ONF, 2004). Although 29 events remain unconfirmed, the reliability of our reconstruction is enhanced by the methodology deployed in this study based on the use of two thresholds for It and GD and the analysis of the spatial repartition of disturbed trees. The two thresholds (i.e. It in 2% of the samples

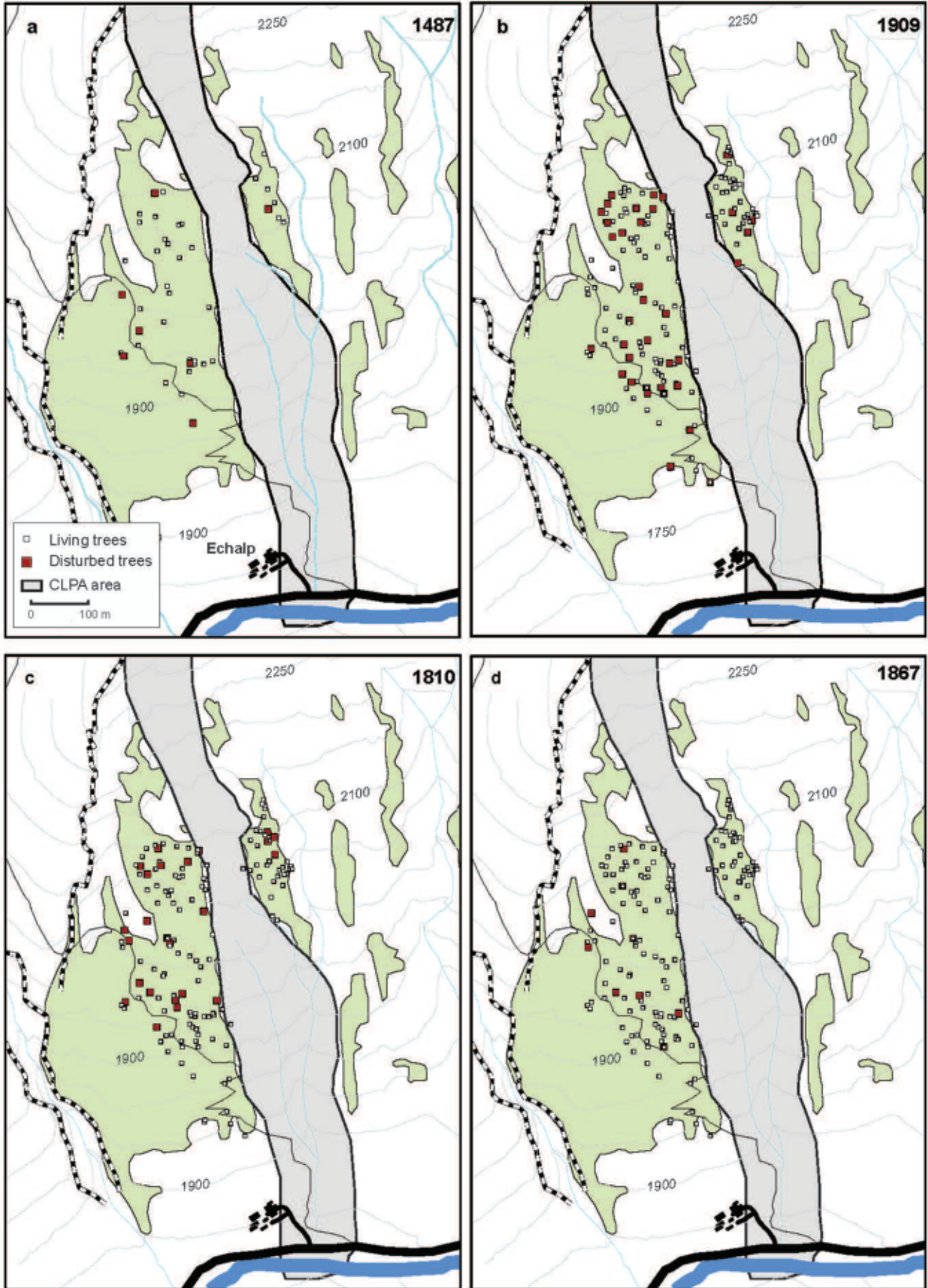


Figure 6. Reconstructed minimum slide extent for the avalanche years of (a) 1487, (b) 1909, (c) 1810 and (d) 1867. Maps show living trees and all trees showing an event-response for the year of the avalanche.

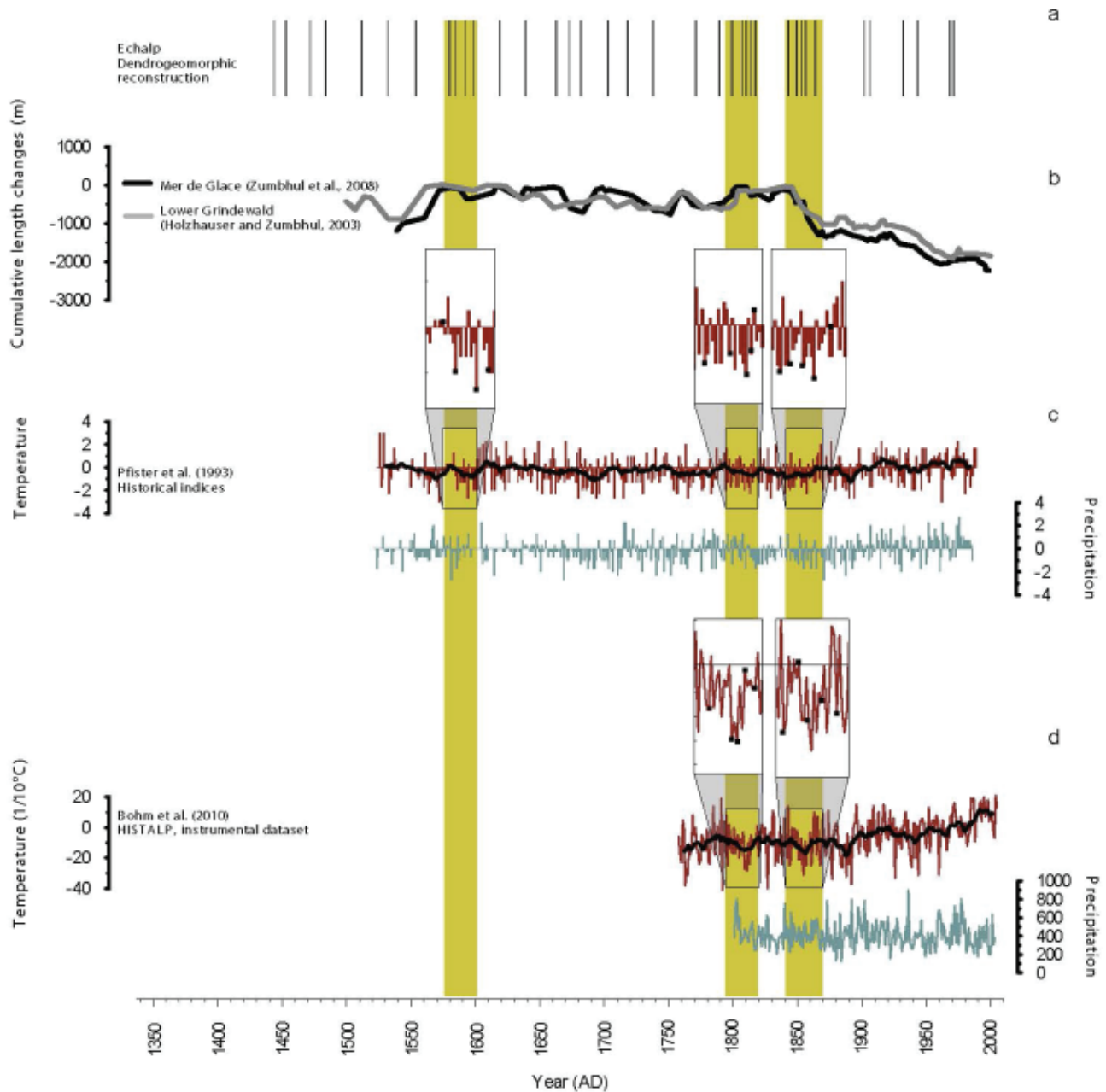


Figure 7. Comparison of reconstructed snow avalanches with (a) the advance/retreat history of the Mer de Glace (Zumbühl et al., 2008) and Lower Grindewald (Holzhauser and Zumbühl, 2005) glaciers, (b) the Pfister historical indices (Pfister, 1993) for winter temperature (in red) and precipitation (in green), (c) the mean series of temperature (in red) and precipitation (in green) computed from the HISTALP dataset (Böhm et al., 2010). Temperature series were smoothed using a 11-year moving average filter (black lines).

present at the time of the event and a minimum number of five trees showing GD) minimized the likelihood that GD resulting from non-avalanche events were included in the chronology (Reardon et al., 2008). The thresholds also facilitated rejection of GD related to other geomorphic processes such as snow creep or rockfall which have been shown to affect a rather limited number of trees per event (Stoffel and Perret, 2006). For years with threshold exceedances, the presence of clear and strong signs of physical impacts (injuries and adjacent callus tissue and/or other severe GD, i.e. intensity 4 and 5 reactions) was used as further criteria for a doubtless dating of snow avalanche events.

However, the comparison between historical archives and tree-ring records at Echalp also shows that dendrogeomorphic techniques failed to confirm five out of the 12 events listed in historical archives. This proportion is comparable with dendrogeomorphic records obtained on an accurately documented path in the Chamonix valley (Corona et al., 2012) and slightly

above the 50% value of unreconstructed events reported by Corona et al. (2010) in the Oisans massif (French Alps).

In any case, the number of reconstructed snow avalanches has to be seen as a minimum frequency of natural avalanche activity, mainly for the following reasons: avalanches have to be of sufficient magnitude to have ecological impacts on trees. Critical snow pressures for stem breakage of trees have been deduced mainly from theoretical models and observational studies (Bartelt and Stöckli, 2001; Bebi et al., 2009) and shown to depend on stem diameter and avalanche type. For flowing avalanches (characterized by a high snow density at the bottom), it can be expected that only events with typical masses $>100 \text{ m}^3$, a path length $>100 \text{ m}$ and an impact pressure $>50 \text{ kPa}$ – i.e. destructive class 2 or larger events according to McClung and Schaerer (1993) or Reardon et al. (2008) – will emerge from the tree-ring record. For powder snow avalanches, critical pressures for an event to be identified in a tree-ring record are lower (3–5 kPa) as

not only the stem but also the crown of a tree is exposed to avalanche pressure (Bebi et al., 2009). Another reason for differences in ecosystem responses of individual trees to snow avalanches are related to tree size and flexibility (Bebi et al., 2009; Kajimoto et al., 2004). A tree flexible enough to be deflected may remain largely undamaged by the avalanche. Small Norway Spruce (*Picea abies* Mill.), *L. decidua* or Cembra pine (*Pinus cembra* L.) trees with heights <5 m and diameters <15–20 cm have been shown to tolerate snow pressure by bending and leaning in the snowpack (Bebi et al., 2009).

In addition, major avalanches may remove or blur the evidence of previous or subsequent events in case that large parts of the forest are destroyed (e.g. Bryant et al., 1989; Carrara, 1979) or that they disturb tree growth in such a way that younger events cannot be identified in the tree-ring record (Kogelnig-Mayer et al., 2011). For example, we find a large number of trees showing GD as a result of the avalanche activity of 1791 but fail to identify the event of 1792 noted in the historical archives. Similarly, the large avalanche of 10 March 1946 destroyed a large portion of the stand in the central part of the path and therefore probably blurred witness of past events that were restricted to a similar zone (MEDD, CEMAGREF, ONF, 2004).

Finally, it seems obvious that the limited number of trees available prior to AD 1450 (<30 trees) will influence the quality of the reconstructed frequency. For the events in 1408 and 1419, referred to as major avalanche years in historical literature, 1 and 2 GD were observed, respectively. However, owing to the strictness of the thresholds used for *It* and GD and the limited number of trees (12 in 1408 and 15 in 1419), these years were rejected from the final reconstruction.

Spatial accuracy of the reconstruction

On a spatial plan, the homogeneous distribution of the oldest trees allows a precise mapping of past events since 1447. The homogeneous stand structure is probably related to human activity as open larch forests were favored and conserved since the end of the Middle Ages for cattle grazing and summer farming (Touflan et al., 2010). Indeed, grass naturally grows under larch forests because of the neutral to slightly acid soils and well-decomposed litter. Moreover, high levels of solar energy can reach the ground, owing to the sparse, soft light foliage of larch and deciduous canopy.

The combination between these dendrogeomorphic maps and historical archives demonstrate that at least 18 events, amongst which six were previously undocumented (in 1740, 1774, 1819, 1846, 1851 and 1909) reached the hamlet of Echalp between 1408 and 1946. Coupling the historical archives and the dendrogeomorphic method, at least one extreme event per century was documented, except for the 16th century. No clear trend could be observed concerning the temporal distribution of these extreme events.

Furthermore, large discrepancies are reported between the lateral limits derived from the dendrogeomorphic approach and the lateral extent of avalanches reported the CLPA. Particularly, all avalanche events reconstructed since 1447 exceeded the lateral limits of the CLPA. For several events, it was usual to identify trees with avalanche damage some 50–100 m outside the CLPA limits. Uncertainties of CLPA boundaries have in fact been evaluated to >50 m (Ancy, 2006; Bonnefoy et al., 2010), albeit, theoretically, CLPA maps should contain the maximum boundaries of historically known avalanches. Yet, these maps are drawn for large areas (scale 1:25,000) and compiled from various sources (historical archives and interviews, field observations and photo interpretation) with often no or only very limited data on the lateral spread of avalanches (Bonnefoy et al., 2010).

Climate influence on avalanche frequency

At the decadal scale, periods of high avalanche activity reconstructed in 1583–1600, 1802–1820, and 1846–1867 match with advances in alpine glaciers. The period 1583–1600 coincides with an almost uninterrupted sequence of cold winters (1583–1595) with only the winters of 1592 and 1594 being slightly above average (Pfister and Brazdil, 1999). According to Casty et al. (2005), very harsh winters occurred at the turn of the 17th century. Temperatures in this interval may have been -2.0°C below the 1901–1960 mean, therefore matching the severity of the periods 1691–1700 and 1886–1895 (Casty et al., 2005; Pfister, 1999[AQ]) which were the coldest decades in Switzerland during the last five centuries.

The other two periods (1802–1820, 1846–1867) coincide with the Dalton and Damon solar minima, respectively. During the Dalton Solar Minimum (1810), a series of tropical eruptions (1808–1815), likely resulted in an aerosol-accumulated cooling effect (Chenoweth, 2001; Dai et al., 1991). This volcanic forcing has been demonstrated to cause a decrease of Northern Hemisphere temperatures on the order of approximately $0.3\text{--}0.6^{\circ}\text{C}$ compared with the reference period of 1961–1990 (Briffa, 2000; Jones et al., 1998). According to regional time series, winters of that period were indeed characterized by a higher frequency of severe climatic conditions than those of the 20th century (Luterbacher et al., 2001). These harsh conditions were found to be partly responsible for glacier advance (Wagner and Zorita, 2005).

These observations are in line with recent findings in the French Alps. Indeed, Castebrunet et al. (2012) observed a bell-shaped pattern in avalanche activity around 1980 coinciding with a short period of colder and snowier winters and glacier advances (Eckert et al., 2011). Similar coincidences between glacier advances and increasing avalanche frequency were reported in western Norway during the ‘Little Ice Age’ (Grove, 1972; Vasskog et al., 2011) and attributed to a general increase in winter precipitation (Nesje et al., 2007).

At the annual scale, the comparison with seasonal Pfister93 and Böhm10 values (Figure 7b, c) confirm the role of temperature on avalanche triggering at Echalp. Interestingly, abnormally cold conditions have also been identified as an aggravating effect for the triggering of the avalanche cycle in December 2008 which led to 42 avalanche events in the Queyras massif (Eckert et al., 2010c). In fact, from 14 to 17 December 2008, a large depression formed over the Mediterranean Sea and maintained a southerly flow of cold air that evolved into a southeasterly flow in eastern France. The heavy snowfalls caused long runouts and an important proportion of destructive powder snow avalanches (Eckert et al., 2010c). Similarly, the avalanche cycle of 1946 was attributed to important snowfalls combined with very cold conditions.

Conversely, no significant correlation was detected between our avalanche reconstruction and winter precipitation. The main limitation for such detection most probably reflects the insufficient spatiotemporal resolution of both data sets. Pfister93 indices were calculated for central Europe. However, as precipitation is spatially and temporally highly variable (e.g. Pauling et al., 2006), large discrepancies may thus exist between snowfalls in the Queyras massif and those in the central Alps. Furthermore, the spatial variability of precipitation could be very important at the Queyras scale. For example, Rousset (1947) reported 10 days of heavy snowfall in the upper Guil valley between 1 and 10 March 1946. More than 3 m of snow dumped on Ristolas resulting in the triggering of an avalanche event at Echalp and in several paths of the upper Guil valley. Conversely, weak snowfalls were reported in other parts of the Queyras massif (Rousset, 1947) and no event was recorded in the historical archives. Finally, the temporal resolution of Böhm10 is probably insufficient to detect situations which might potentially lead to the triggering of snow avalanches. Indeed, the

3- to 10-day snowfalls are involved as main explanatory factors for the avalanche cycles of February 1946 and December 2008 in the Queyras massif (Eckert et al., 2010c; Rousset, 1947; Sanson, 1948). Such exceptional snowfalls may be difficult to detect in seasonal series. For example, despite heavy snowfalls in March 1946, the winter of 1945–1946, is on average of the period 1961–1990, as a result of scarce precipitation between December 1945 and the end of February 1946.

Conclusion

In mountain areas such as the Alps, the increase in human activity has resulted in increased risks for natural hazards such as snow avalanches. Therefore, it has become imperative to improve avalanche forecasting at the local level. Nevertheless, because anticipated changes in climate may alter the dynamics of slope processes and the frequency or magnitude of extreme events, understanding the mechanisms that link climate and avalanche activity is the first step in any attempt at forecasting. In that respect, analyses based on long historical records of avalanche occurrences can be very useful for improving avalanche prediction.

This study demonstrates that, in multicentennial stands, dendrogeomorphic methods clearly have the potential to reconstruct past avalanche events for several centuries and to add substantially to the historic record. Furthermore, the maxima detected in snow avalanche frequency are correlated with glacier advances and below average temperature, thus confirming the existence of a climatic signal in avalanche frequency fluctuations.

In addition, dendrogeomorphic data can add evidence to the extent of past events where other sources often fail to produce conclusive results. The method enables an accurate mapping of events. The comparison with the CLPA clearly demonstrates that it adds evidence on the runout distance of large events and that the lateral spread of past avalanches can be better defined. Nonetheless, assessing the result of this study, particularly concerning the effect of recent climate change, could be accomplished by (1) replicating studies for a larger number of avalanche paths in order to improve the significance of the observed trends and (2) using weather station instrumentation at remote sites, calibrated against long meteorological time series, to obtain more relevant data for modeling.

Funding

This research received no specific grant from any funding agency in the public, commercial or not-for-profit sectors.

References

- Alestalo J (1971) Dendrochronological interpretation of geomorphic processes. *Fennia* 105: 1–139.
- Ancey C (2006) *Dynamique des avalanches*. Lausanne: Presses polytechniques et universitaires Romandes, 352 pp.
- Bartelt P and Stöckli V (2001) The influence of tree and branch fracture, overturning and debris entrainment on snow avalanche flow. *Annals of Glaciology* 32: 209–216.
- Bebi P, Kulakowski D and Rixen C (2009) Snow avalanche disturbances in forest ecosystems – State of research and implications for management. *Forest Ecology and Management* 257: 1883–1892.
- Blikra LH and Selvik SF (1998) Climatic signals recorded in snow avalanche-dominated colluvium in western Norway: Depositional facies successions and pollen records. *The Holocene* 8: 631–658.
- Böhm R, Jones PD, Hiebl J et al. (2010) The early instrumental warm-bias: A solution for long central European temperature series 1760–2007. *Climate Change* 101: 41–67.
- Bonnefoy M, Escande S, Cabos S et al. (2010) Localization map of avalanche phenomena (CLPA) and collection of eye witness accounts: Field investigation method, biases, alternatives and limits, data quality. In: Gleason JA (ed.) *Proceedings of the International Snow Science Workshop*. 17–22 October, Squaw Valley CA.
- Briffa KR (2000) Annual climate variability in the Holocene: Interpreting the message of ancient trees. *Quaternary Science Review* 19: 87–105.
- Bryant CL, Butler DR and Vitek JD (1989) A statistical analysis of tree-ring dating in conjunction with snow avalanches: Comparison of on-path versus off-path responses. *Environmental Geology and Water Sciences* 14: 53–59.
- Butler DR (1987) Teaching general principles and applications of dendrogeomorphology. *Journal of Geological Education* 35: 64–70.
- Butler DR and Malanson GP (1985) A history of high-magnitude snow avalanches, Southern glacier national park, Montana, U.S.A. *Mountain Research and Development* 5: 175–182.
- Butler DR and Sawyer CF (2008) Dendrogeomorphology and high-magnitude snow avalanches: A review and case study. *Natural Hazards and Earth System Science* 8: 303–309.
- Butler DR, Sawyer CF and Maas JA (2010) Tree-ring dating of snow avalanches in Glacier National Park, Montana, USA In: Stoffel M, Bollschweiler M, Butler DR et al. (eds) *Tree Rings and Natural Hazards*. Dordrecht: Springer, pp. 33–44.
- Carrara PE (1979) The determination of snow avalanche frequency through tree-ring analysis and historical records at Ophir, Colorado. *Geological Society of America Bulletin* 90: 773.
- Castebrunet H, Eckert N and Giraud G (2012) Snow and weather climatic control on snow avalanche fluctuations over 50yr in French Alps. *Climate of the Past* 8: 855–875.
- Casteller A, Stöckli V, Villalba R et al. (2007) An evaluation of dendroecological indicators of snow avalanches in the Swiss Alps. *Arctic, Antarctic, and Alpine Research* 39: 218–228.
- Casteller A, Villalba R, Araneo D et al. (2011) Reconstructing temporal patterns of snow avalanches at Lago del Desierto, Southern Patagonian Andes. *Cold Regions Science and Technology* 67: 68–78.
- Casty C, Wanner H, Luterbacher J et al. (2005) Temperature and precipitation variability in the European Alps since 1500. *International Journal of Climatology* 25: 1855–1880.
- Chenoweth M (2001) Two major volcanic cooling periods derived from global marine air temperature, AD 1807–1827. *Geophysical Research Letters* 28: 2963–2966.
- Corona C, Lopez Saez J, Stoffel M et al. (2012) How much of the real avalanche activity can be captured with tree rings? An evaluation of classic dendrogeomorphic approaches and comparison with historical archives. *Cold Science Region and Technology* doi:10.1016/j.coldregions.2012.01.003.
- Corona C, Rovéra G, Lopez Saez J et al. (2010) Spatio-temporal reconstruction of snow avalanche activity using tree rings: Pierres Jean Jeanne avalanche talus, Massif de l'Oisans, France. *Catena* 83: 107–118.
- Dai J, Mosley-Thompson E and Thompson LG (1991) Ice core evidence for an explosive tropical volcanic eruption six years preceding Tambora. *Journal of Geophysical Research* 96: 17,361–17,366.
- Dubé S, Filion L and Héty B (2004) Tree-ring reconstruction of high-magnitude snow avalanches in the Northern Gaspé Peninsula, Québec, Canada. *Arctic, Antarctic, and Alpine Research* 36: 555–564.
- Eckert N, Baya H and Deschatres M (2010a) Assessing the response of snow avalanche runout altitudes to climate fluctuations using hierarchical modeling: Application to 61 winters of data in France. *Journal of Climate* 23: 3157–3180.
- Eckert N, Baya H, Thibert E et al. (2011) Extracting the temporal signal from a winter and summer mass-balance series: Application to a six-decade record at Glacier de Sarennes, French Alps. *Journal of Glaciology* 57: 134–150.
- Eckert N, Coleou C, Castebrunet H et al. (2010c) Cross-comparison of meteorological and avalanche data for characterising avalanche cycles: The example of December 2008 in the eastern part of the French Alps. *Cold Regions Science and Technology* 64: 119–136, doi:10.1016/j.coldregions.2010.08.009.
- Eckert N, Parent E, Kies R et al. (2010b) A spatio-temporal modelling framework for assessing the fluctuations of avalanche occurrence resulting from climate change: Application to 60 years of data in the northern French Alps. *Climatic Change* 101: 515–553, doi:10.1007/s10584-009-9718-8.
- Fliri F (1998) *Naturchronik von Tirol: Tirol, Oberpinzgau, Vorarlberg, Trentino: Beiträge zur Klimatographie von Tirol*. Innsbruck: Universitätsverlag Wagner, 369 pp.
- Germain D, Filion L and Héty B (2009) Snow avalanche regime and climatic conditions in the Chic-Choc Range, eastern Canada. *Climatic Change* 92: 141–167.
- Grove JM (1972) The incidence of landslides, avalanches, and flood in western Norway during the Little Ice Age. *Arctic and Alpine Research* 4: 131–138.
- Holmes RL (1983) Computer-assisted quality control in tree-ring dating and measurement. *Tree-Ring Bulletin* 43: 69–75.

- Holzhauser H, Magny M and Zumbühl HJ (2005) Glacier and lake-level variations in west-central Europe over the last 3500 years. *The Holocene* 15: 789–801.
- Johnson EA (1987) The relative importance of snow avalanche disturbance and thinning on canopy plant populations. *Ecology* 68: 43–53.
- Jomelli V and Pech P (2004) Effects of the Little Ice Age on avalanche boulder tongues in the French Alps (Massif des Ecrins). *Earth Surface Processes and Landforms* 29: 553–564.
- Jones PD, Briffa KR, Barnett TP et al. (1998) High-resolution palaeoclimatic records for the past millennium: Interpretation, integration and comparison with general circulation model control-run temperatures. *The Holocene* 8: 455–471.
- Kajimoto T, Daimaru H, Okamoto T et al. (2004) Effects of snow avalanche disturbance on regeneration of subalpine *Abies mariesii* forest, Northern Japan. *Arctic, Antarctic, and Alpine Research* 36: 436–445.
- Kogelnig-Mayer B, Stoffel M, Bollschweiler M et al. (2011) Possibilities and limitations of dendrogeomorphic time-series reconstructions on sites influenced by debris flows and frequent snow avalanche activity. *Arctic, Antarctic, and Alpine Research* 43: 649–658.
- Laely A (1984) *Davoser Heimatkunde. Beiträge zur Geschichte der Landschaft Davos. 2. Auflage*. Davos: Verlag Genossenschaft Davoser Revue, 275 pp.
- Laternser M and Schneebeli M (2002) Temporal trend and spatial distribution of avalanche activity during the last 50 years in Switzerland. *Natural Hazards* 27: 201–230.
- Le Gallou JY and Guignard P (2011) *Modalité de prise en compte des avalanches exceptionnelles pour améliorer la prévention des risques et renforcer la sécurité des personnes*. Rapport no.007395–01, Conseil Général de l'Environnement et du Développement durable, 86 pp.
- Lemoine M and Tricart P (1986) Les schistes lustrés piémontais des Alpes occidentales: approche stratigraphique, structurale et sédimentologique. *Eclogae geologicae Helvetiae* 79: 271–294.
- Luckman BH (2010) Dendrogeomorphology and snow avalanche research. In: Stoffel M, Bollschweiler M, Butler DR et al. (eds) *Tree Rings and Natural Hazards. A State-of-the-Art*. Dordrecht, Heidelberg, London, New York: Springer, pp. 27–34.
- Luterbacher J, Rickli R, Xoplaki E et al. (2001) The late Maunder Minimum (1675–1715) – A key period for studying decadal scale climate change in Europe. *Climatic Change* 49: 441–462.
- McCarroll D (1993) Modelling late-Holocene snow-avalanche activity: Incorporating a new approach to lichenometry. *Earth Surface Processes and Landforms* 18: 527–539.
- McCarroll D, Matthews JA and Shakesby RA (1995) Late-Holocene snow-avalanche activity in southern Norway: Interpreting lichen size-frequency distributions using an alternative to simulation modelling. *Earth Surface Processes and Landforms* 20: 465–471.
- McClung D and Schaerer P (1993) *The Avalanche Handbook*. Seattle: Mountaineers.
- Malanson P and Butler DR (1984) Transverse pattern of vegetation on avalanche paths in the northern Rocky Mountains, Montana. *Western North American Naturalist* 44: 453–458.
- MEDD, CEMAGREF, ONF (2004) *Notice sur les avalanches constatées et leur environnement dans le massif du Queyras*. CLPA-Notice par massif, 6 pp.
- Moran PAP (1950) Notes on continuous stochastic phenomena. *Biometrika* 37: 17–23.
- Muntan E, Andreu L, Oller P et al. (2004) Dendrochronological study of the Canal del Roc Roig avalanche path: First results of the Aludex project in the Pyrenees. *Annals of Glaciology* 38: 173–179.
- Muntan E, Garcia C, Oller P et al. (2009) Reconstructing snow avalanches in the Southeastern Pyrenees. *Natural Hazards and Earth System Science* 9: 1599–1612.
- Nesje A, Bakke J, Dahl, SO et al. (2007) A continuous high-resolution 8500-yr snow avalanche record from western Norway. *The Holocene* 17: 269–277.
- Pauling A, Luterbacher J, Casty C et al. (2006) Five hundred years of gridded high-resolution precipitation reconstructions over Europe and the connection to large-scale circulation. *Climate Dynamics* 26: 387–405.
- Pfister C (1993) *Historical Weather Indices from Switzerland*. IGBP PAGES/World Data Center-A for Paleoclimatology Data Contribution Series #93–027. Boulder CO: NOAA/NGDC Paleoclimatology Program.
- Pfister C (1999) *Wetternachhersage. 500 Jahre Klimavariationen und Naturkatastrophen 1496–1995*. Bern: Haupt, 304 pp.
- Pfister C and Brazdil R (1999) Climatic variability in sixteenth-century Europe and its social dimension: A synthesis. *Climatic Change* 34: 91–108.
- Potter N (1969) Tree-ring dating of snow avalanche tracks and the geomorphic activity of avalanches, northern Absaroka Mountains, Wyoming, Boulder, CO. *Geological Society of America Special Paper* 123: 141–165.
- Reardon BA, Pederson GT, Caruso CJ et al. (2008) Spatial reconstructions and comparisons of historic snow avalanche frequency and extent using tree rings in Glacier National Park, Montana, U.S.A. *Arctic, Antarctic, and Alpine Research* 40: 148–160.
- Rinntech (2009) <http://www.rinntech.com/content/blogcategory/2/28/lang,english/>
- Rousset R (1947) L'enneigement de printemps dans les Alpes du nord en 1946. *Revue de Géographie Alpine* 35: 119–121.
- Sanson J (1948) Les principales anomalies météorologiques de l'année 1947 en France. *Annales de Géographie* 57: 178–181.
- Schaerer P (1972) Terrain and vegetation of snow avalanche sites at Rogers Pass, British Columbia. In: Slaymaker O and McPherson HJ (eds) *Mountain Geomorphology: Geomorphological Processes in the Canadian Cordillera*. Vancouver BC: Tantalus Research Ltd edition, pp. 215–222.
- Schneebeli M, Laternser M and Ammann W (1997) Destructive snow avalanches and climate change in the Swiss Alps. *Eclogae Geologicae Helvetiae* 90: 457–461.
- Schneuwly DM, Stoffel M and Bollschweiler M (2008) Formation and spread of callus tissue and tangential rows of resin ducts in *Larix decidua* and *Picea abies* following rockfall impacts. *Tree Physiology* 29: 281–289.
- Shroder J (1980) Dendrogeomorphology; review and new dating techniques of tree-ring dating. *Progress in Physical Geography* 4: 161–188.
- Stoffel M and Bollschweiler M (2008) Tree-ring analysis in natural hazards research – An overview. *Natural Hazards and Earth System Science* 8: 187–202.
- Stoffel M and Bollschweiler M (2009) What tree rings can tell about earth-surface processes. Teaching the principles of dendrogeomorphology. *Geography Compass* 3: 1013–1037.
- Stoffel M and Hitz OM (2008) Snow avalanche and rockfall impacts leave different anatomical signatures in tree rings of *Larix decidua*. *Tree Physiology* 28(11): 1713–1720.
- Stoffel M and Perret S (2006) Reconstructing past rockfall activity with tree rings: Some methodological considerations. *Dendrochronologia* 24: 1–15.
- Stoffel M, Bollschweiler M, Butler DR et al. (2010) *Tree Rings and Natural Hazards: A State-of-the-Art*. Dordrecht, New York: Springer.
- Stoffel M, Bollschweiler M and Hassler GR (2006) Differentiating past events on a cone influenced by debris-flow and snow avalanche activity – A dendrogeomorphological approach. *Earth Surface Processes and Landforms* 31(11): 1424–1437.
- Timell TE (1986) *Compression Wood in Gymnosperms*. Berlin: Springer-Verlag.
- Tivollier J and Inel P (1938) *Le Queyras (Hautes-Alpes)*. Marseille: Laffite Reprints, 498 pp.
- Touflan P, Talon B and Walsh K (2010) Soil charcoal analysis: A reliable tool for spatially precise studies of past forest dynamics: A case study in the French southern Alps. *The Holocene* 20: 44–52.
- Vasskog K, Nesje A, Nage E et al. (2011) A Holocene record of snow avalanche and flood activity reconstructed from a lacustrine sedimentary sequence in Oldevatnet, western Norway. *The Holocene* DOI: 10.1177/0959683610391316.
- Wagner S and Zorita E (2005) The influence of volcanic, solar and CO₂ forcing on the temperatures in the Dalton Minimum (1790–1830): A model study. *Climate Dynamics* 25: 205–218.
- Zumbühl H, Steiner D and Nussbaumer S (2008) 19th century glacier representations and fluctuations in the central and western European Alps: An interdisciplinary approach. *Global and Planetary Change* 60: 42–57.